AIP | APL Materials
NOW INDEXED IN THOMSON REUTERS DATABASES

Hydrogen plasma treatment for improved conductivity in amorphous aluminum doped zinc tin oxide thin films

M. Morales-Masis, L. Ding, F. Dauzou, Q. Jeangros, A. Hessler-Wyser, S. Nicolay, and C. Ballif

Citation: APL Materials **2**, 096113 (2014); doi: 10.1063/1.4896051
View online: http://dx.doi.org/10.1063/1.4896051
View Table of Contents: http://scitation.aip.org/content/aip/journal/aplmater/2/9?ver=pdfcov
Published by the AIP Publishing

APL MATERIALS **2**, 096113 (2014)

Hydrogen plasma treatment for improved conductivity in amorphous aluminum doped zinc tin oxide thin films

M. Morales-Masis,[1,a] L. Ding,[1] F. Dauzou,[1] Q. Jeangros,[2] A. Hessler-Wyser,[1,2] S. Nicolay,[3] and C. Ballif[1,3]

[1]*Photovoltaics and Thin-Film Electronics Laboratory (PVLab), Institute of Microengineering (IMT), Ecole Polytechnique Fédérale de Lausanne (EPFL), Rue de la Maladière 71b, CH-2002 Neuchatel, Switzerland*

[2]*Interdisciplinary Centre for Electron Microscopy, Ecole Polytechnique Fédérale de Lausanne (EPFL), Lausanne, Switzerland*

[3]*Centre Suisse d'Electronique et de Microtechnique (CSEM) SA, Rue Jaquet-Droz 1, CH-2002 Neuchatel, Switzerland*

(Received 3 August 2014; accepted 8 September 2014; published online 18 September 2014)

Improving the conductivity of earth-abundant transparent conductive oxides (TCOs) remains an important challenge that will facilitate the replacement of indium-based TCOs. Here, we show that a hydrogen (H_2)-plasma post-deposition treatment improves the conductivity of amorphous aluminum-doped zinc tin oxide while retaining its low optical absorption. We found that the H_2-plasma treatment performed at a substrate temperature of 50 °C reduces the resistivity of the films by 57% and increases the absorptance by only 2%. Additionally, the low substrate temperature delays the known formation of tin particles with the plasma and it allows the application of the process to temperature-sensitive substrates. [http://dx.doi.org/10.1063/1.4896051]

Due to their compatibility with low-temperature deposition methods and their high mobility compared to amorphous silicon (a-Si), amorphous transparent conductive oxides (TCOs) have been widely studied in the past 10 years for application in flexible and transparent thin-film transistors.[1–4] The amorphous nature of these TCOs also ensures very smooth surface morphologies useful for electrodes in polymer and organic light-emitting devices (OLEDs).[5] Amorphous zinc tin oxide (a-ZTO) compounds are interesting oxide materials since zinc (Zn) and tin (Sn) are inexpensive, abundant, and non-toxic, however this compound presents the disadvantage of low conductivity. Enhancing its conductivity remains a challenge in the TCO community and represents a significant step towards the replacement of scarce indium-containing oxides, like indium tin oxide (ITO). Additionally, a-ZTO compounds present extremely high thermal and chemical stability.[6–8] Their high resistance to wet etching processes is an advantage over zinc oxide (ZnO), and their insolubility in acid solutions commonly used for patterning is an advantage over, e.g., indium-gallium-zinc oxide (IGZO).[9]

Hydrogen is known to act as a shallow electron donor in several conductive oxide materials, either in interstitial positions (H_i) or on an oxygen site (H_o).[10–13] Specifically for a-ZTO, it has been proposed that hydrogen introduction during the sputtering deposition increases the carrier concentration of the films.[14] Korner *et al.* proposed that hydrogen doping suppresses deep band defects improving the optical properties of ZTO films.[15] Hydrogen (H_2) plasma treatments have already been applied to a-TCOs,[16,17] however, mainly in solution-processed TCOs this treatment is usually accompanied by a high temperature annealing step, making it unsuitable for flexible substrates.[16] In Sn- and In-based TCOs, it is also known that the H_2 plasma leads to the formation

[a]Author to whom correspondence should be addressed. Electronic mail: monica.moralesmasis@epfl.ch

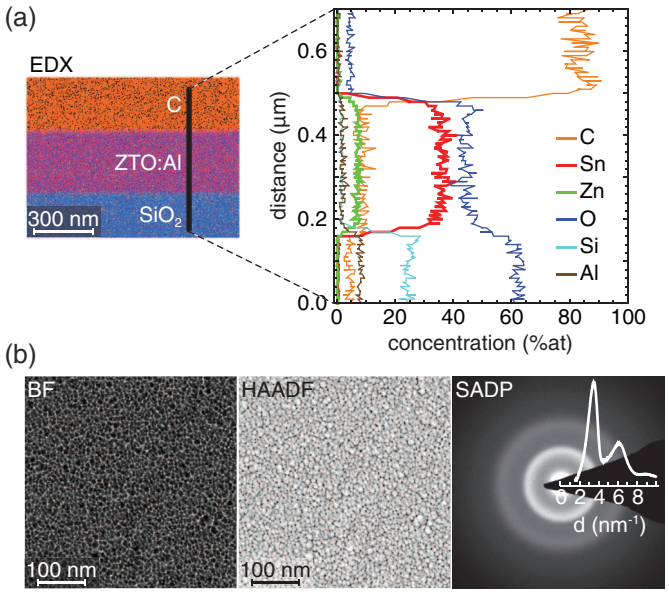

FIG. 1. (a) Composition profile of an as-prepared a-ZTO:Al layer determined by STEM EDX. (b) BF and HAADF plan-view of the films. The SAD pattern indicates that the layers are amorphous.

of metal particles which deteriorate the optical transmittance and therefore, an additional etching step is required to remove these particles.[16–19] In this paper, we show how controlling the H_2 plasma process parameters we increase the free-electron concentration of amorphous aluminium-doped zinc tin oxide (a-ZTO:Al) while delaying the formation of Sn particles, avoiding with it the additional process step to remove the particles. In addition, this process is performed at substrate temperatures lower than 200 °C making it compatible for applications on low cost plastic flexible substrates.

The studied a-ZTO:Al films were co-sputtered from SnO_2 and ZnO:Al (2 wt. % Al_2O_3) targets by RF magnetron sputtering in an Oerlikon Clusterline System. The rf power density was 5.1 W/cm^2 for the SnO_2 target and 1.9 W/cm^2 for the ZnO:Al target. The co-sputtering deposition was performed at a process pressure of 5.5×10^{-3} mbar with an oxygen to total flow ratio, $r(O_2) = O_2/(Ar + O_2)$, of 0.34%. All samples were deposited at 60 °C onto glass substrates (4 × 8 cm). The deposition rate was of 0.5 nm/s and the sputtering time was adjusted to obtain films with a thickness of 300 ± 10 nm. The structural properties of the layers were characterized by X-ray diffraction (XRD) and transmission electron microscopy (TEM). For the TEM examination, the cross-sections were prepared by a conventional focused ion beam (FIB) lift-out technique (Zeiss Nvision) and for the top-view imaging dedicated 150-nm-thick layers were grown on carbon grids. The crystallographic properties of the films were determined using selected area diffraction (SAD), while the structural assessment of the films involved the acquisition of scanning TEM (STEM) bright-field (BF) and high-angle annular dark-field (HAADF) images. The chemical composition of the films was determined by Rutherford backscattering (RBS) and STEM energy-dispersive X-ray spectroscopy (EDX). The chemical composition depth profile was also measured by secondary ion mass spectrometry (SIMS) with a Cs^+ primary ion source, negative secondary ion detection for H and C and positive secondary ion detection for Zn, Sn, and O. Hall mobility (μ_{Hall}), free-carrier concentration (N_e), and resistivity (ρ) were determined by Hall-effect measurements using the van der Pauw configuration. Optical transmittance and reflection spectra in the range of 320 to 1750 nm were measured using a UV-Vis-NIR spectrophotometer equipped with an integrating sphere. The absorptance was calculated from the total transmittance and reflectance spectra.

Figure 1 presents the STEM EDX, HAADF, and BF analyses of as-prepared ZTO layers. As can be observed in Fig. 1(a), the Sn/Zn atomic ratio was constant across the thickness of the layer and equals to Sn/Zn = 4.2. In agreement, RBS measurements indicate that the film composition (Zn(at. %), Sn(at. %), and O(at. %)) is 6.3%, 27.8%, and 65.9%, respectively. The Al content was

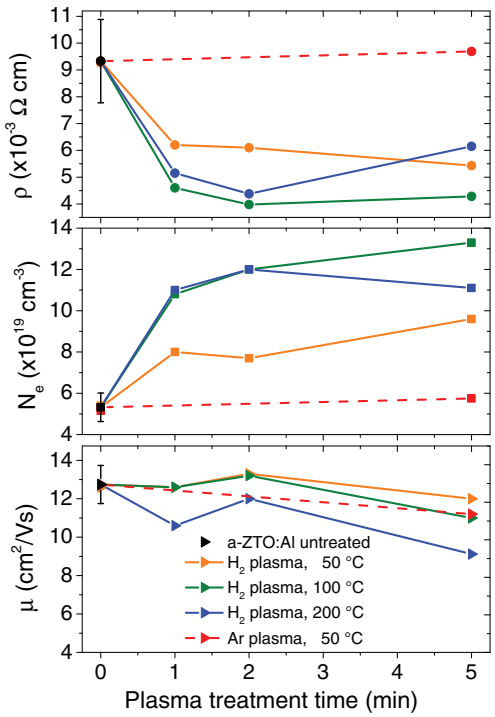

FIG. 2. Free-carrier concentration (N_e) and Hall mobility (μ_{Hall}) as a function of H_2 plasma exposure time for substrate temperatures of 50, 100 and 200 °C. The lines are only guidance for the eyes.

not detected with RBS, however, its presence in the film was confirmed with SIMS (supplementary material, Fig. S1).[21] The SAD pattern (Fig. 1(b)) clearly shows that the material is amorphous, showing no more structure than broad first and second nearest neighbor peaks. The amorphous phase was also confirmed by XRD measurements.

The as-deposited a-ZTO:Al thin films present a ρ of 9×10^{-3} Ω cm, N_e of 5×10^{19} cm^{-3} and μ_{Hall} of 13 cm^2/V s. The optical transmittance of the films averaged over the range of 390–800 nm is 80%. The average absorptance over the same range is 4%.

A H_2 plasma treatment was applied to the a-ZTO:Al films using a RF source with a power density of 0.12 W cm^{-2}. The base pressure was set to 0.5 mbar under a constant flow of H_2 gas. Figure 2 presents the changes in ρ, N_e, and μ_{Hall} after H_2 plasma treatments with different substrate temperatures (T_s) and exposure times.

As the H_2 plasma treatment time increases, N_e increases for all T_s (50, 100, and 200 °C). The plasma treatment at 50 °C presents a slower rate of increase than the treatments at 100 and 200 °C. After 1 min of exposure to the H_2 plasma, the N_e of the samples treated at 100 and 200 °C reaches values higher than 1×10^{20} cm^{-3}, while for the sample treated at 50 °C, N_e is 8×10^{19} cm^{-3} after 1 min and close to 1×10^{20} cm^{-3} after 5 min. The lowest ρ reached is of 3.9×10^{-3} Ω cm for the sample treated at 100 °C. μ_{Hall} drops slightly, mainly for the sample treated at 200 °C.[20]

In order to verify that the strong increase in N_e observed after the H_2 plasma treatment can be ascribed to the ionized H^+ and not to the plasma in general (for example, exposure to ultraviolet light), we also performed the plasma treatment at 50 °C using argon (Ar) as the working gas. As observed in Fig. 2, after 5 min of treatment, N_e does not present any significant increase as compared to the H_2 plasma treatment.

In terms of optical properties (Fig. 3), we observe an increase in free-carrier absorption for wavelengths higher than 800 nm, associated with the increase in N_e. In the visible range, we observe the appearance of a feature at around 550 nm which amplitude progressively increases and is red-shifted with exposure time and T_s. We ascribe this feature to a plasmon resonance peak, due to the formation of Sn metallic particles at the surface of the film.[21] We further ascribe its red-shift

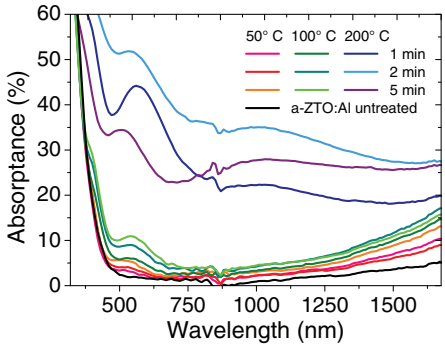

FIG. 3. Absorptance spectra of the untreated and H_2-plasma treated a-ZTO:Al films as a function of H_2-plasma exposure time and T_s. The absorptance of the Ar-plasma treated a-ZTO:Al (not shown) at 50 °C remains equal to that of the untreated film.

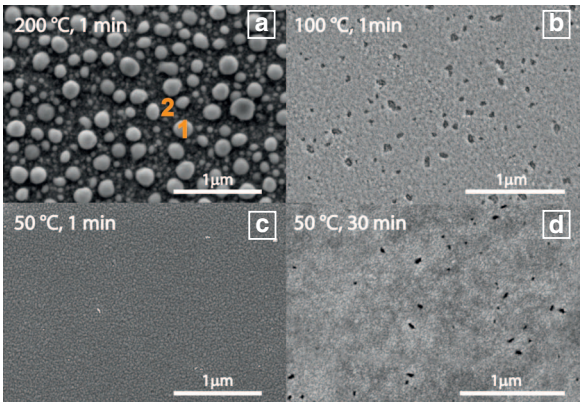

FIG. 4. Top-view SEM micrographs of a-ZTO:Al samples treated for 1 min in a H_2-plasma at T_s = (a) 200, (b) 100, and (c) 50 °C. The numbers 1 and 2 indicate spots measured by EDX. The results in at. % are: Area 1: O 27, Zn 1.6, Sn 71; Area 2: O 65, Zn 6.5, Sn 28.7. (d) a-ZTO:Al samples treated for 30 min in a H_2-plasma at T_s = 50 °C. The surface of the layer shows the same morphology as the sample treated at 100 °C for 1 min.

to the increase in size of the Sn particles. This was confirmed with SEM micrographs of the films before and after H_2 plasma exposure. Figure 4 shows the clear formation of Sn metallic particles with diameters in the range of 100 nm on the surface of the samples treated at a T_s of 200 °C. For the samples treated at 100 °C for 1 min and at 50 °C for 30 min only the onset of particle formation is visible, and for the samples treated at 50 °C for 1 min the particles are not detectable with SEM.

Similar optical effects caused by surface plasmon resonances at metallic nanoparticles have been reported for other oxide materials. Albrecht *et al.* reported surface plasmon resonances at metallic indium nanoparticles embedded in In_2O_3 films.[22] For the specific case of Sn nanoparticles 107 nm in diameter and 52 nm in height embedded in SiO_2, a rather broad resonance peak at around 620 nm was reported.[23]

To increase the conductivity of the a-ZTO:Al films while retaining low optical absorptance, the films were exposed to the H_2 plasma at 50 °C for longer times. As presented in Fig. 5, after 30 min of exposure, N_e reaches 1.3×10^{20} cm^{-3}. This is the same value achieved with 5 min H_2 plasma at 100 °C. However, the treatment at 50 °C still presents an advantage in optical absorptance: 6% for the 50 °C 30-min H_2 plasma compared to 9.5% for the 100 °C 5-min H_2 plasma, both values averaged in the range of 390–800 nm. The surface morphology of the films after 30 min of plasma treatment is presented in Fig. 4(d).

We measured the electrical and optical properties of the H_2-plasma-treated a-ZTO:Al up to several months after the treatment, and no changes were found, confirming that the effects of the treatment are highly stable.

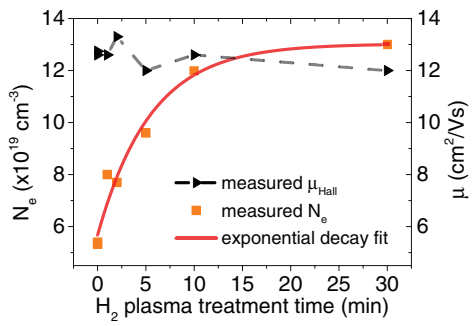

FIG. 5. Free-carrier concentration (N_e) and Hall mobility (μ_{Hall}) as a function of H_2 exposure time at a T_s of 50 °C. The red curve represents the exponential decay fit with Eq. (6).

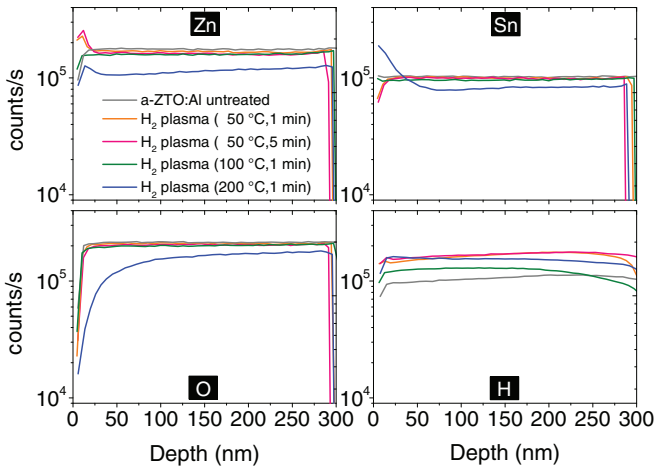

FIG. 6. SIMS depth profiles for Zn, Sn, O, and H measured in the H_2-plasma-treated and untreated a-ZTO:Al thin films.

SIMS measurements were performed on the untreated and on the H_2-plasma-treated samples to investigate possible changes in the chemical composition depth profiles before and after treatment, as well as to check the possible introduction of H ions into the a-ZTO:Al films. The depth profiles for Zn, Sn, O, and H are presented in Fig. 6.

The depth profiles of the untreated samples and of the samples treated at 50 and 100 °C show a uniform distribution of Zn, Sn, and O across the thickness of the layers (the first 10 nm of the measured profiles are not considered in the analysis because of possible side effects induced by the ions used for the sputtering during SIMS). The sample treated at 200 °C shows a clear depletion of oxygen that increases towards the surface of the film. The same sample also shows an increase in the Sn signal close to the surface of the a-ZTO:Al. This corresponds well with the high density of Sn metallic particles present on the a-ZTO:Al after the treatment at 200 °C.

The H concentration profiles of the untreated and H_2-plasma-treated samples also show a relatively uniform distribution across the thickness of the layers. Only a slightly higher content of H is measured for the samples treated with the H_2-plasma, as compared with the untreated sample. This suggests a very limited introduction of H into the layers or a relatively similar rate of H absorption and desorption (as O–H radicals or H_2O) during the H_2 plasma treatment. The source of the H already present in the as-deposited films could be attributed to H-species introduced directly from the deposition, for example, residual H in the sputtering target or sputtering chamber.[24] "Hidden" H is also known to be present in ZnO and SnO_2 samples.[25]

From the SIMS measurements we do not observe a significant increase of H content after the H_2 plasma treatment, suggesting that interstitial hydrogen (H_i) or hydrogen at oxygen vacancies (H_o), are unlike to be the cause of the increased N_e. In addition, the high stability over time of the

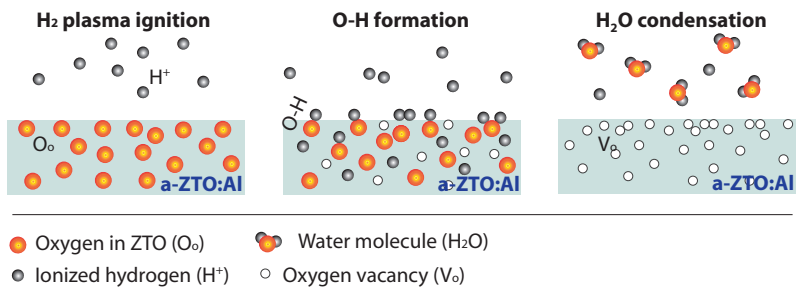

FIG. 7. Schematic diagram illustrating the proposed mechanism responsible for the formation of oxygen vacancies at the a-ZTO:Al surface during H_2 plasma exposure.

effects of the H_2 plasma on our a-ZTO:Al samples (i.e., the increase in N_e) supports the fact that H_i (a non-thermally stable defect) is not the source of increased N_e.[10,25]

Hydrogen is a highly reducing agent and can therefore easily reduce O from the a-ZTO:Al following the chemical reaction,

$$O_o + 2H \rightarrow V_O{}^{2+} + 2e^- + H_2O. \tag{1}$$

Consequently, as represented in Fig. 7, an alternative explanation of the increase in N_e is that oxygen vacancies may be created by the assisted reduction of O following reaction (1). The ionized H^+ reacts with oxygen atoms of the a-ZTO:Al to form OH radicals. These groups are highly reactive and therefore immediately find another free H^+ to form a H_2O molecule, which then desorbs to the gas phase. We suggest that this process is responsible for the removal of oxygen from the a-ZTO:Al, forming doubly charged oxygen vacancies ($V_O{}^{2+}$). The creation of $V_O{}^{2+}$ liberates two electrons, therefore increasing the overall N_e.[4,26–28]

Due to the formation of $V_O{}^{2+}$, Sn^{+4} is destabilized and reduced to its metallic state. This represents the possible second chemical reaction occurring during the H_2 plasma treatment,

$$Sn^{+4} + 4e^- \rightarrow Sn. \tag{2}$$

Following Albrecht *et al.*,[22] we propose that this second reaction occurs only after a critical concentration of V_O is formed in the film. The formation of Sn metallic particles is responsible for the deterioration of the optical properties of the films. Note that the reduction of Zn is ignored in this discussion based on the fact that ZnO is known to be more stable under reducing atmospheres than SnO_2[29,30] and based on the EDX analysis of the samples treated at 200 °C presented in Fig. 4.

Following reaction (1), the rate of formation of $V_O{}^{2+}$ would then depend on the rate of O_o reduction and desorption from the a-ZTO:Al. This process can be described by a first-order reaction kinetics expressed as

$$\frac{-d[O_o]}{dt} = \frac{d[V_O^{+2}]}{dt} = k[V_O^{+2}]. \tag{3}$$

Considering that the measured increase in N_e is proportional to $[V_O^{+2}]$,

$$\frac{d[V_O^{+2}]}{dt} \propto \frac{d[N_e']}{dt} = k[N_e']. \tag{4}$$

This differential equation has the solution

$$N_e' = N_{e0}' \exp(-kt) \tag{5}$$

with k the reaction rate constant. Using, $N_e' = N_{e,final} - N_{e,meas}$, with $N_{e,meas}$ the measured N_e and $N_{e,final}$ the maximum N_e of 1.3×10^{20} cm^{-3},

$$N_{e,meas} = N_{e,final} - N_{e0}' \exp(-kt). \tag{6}$$

Using Eq. (6), we fit the data presented in Fig. 5 of N_e *versus* t (red curve). The fit shows excellent agreement with the experimental data. This exponential decay behaviour indicates that the increase

in N_e reach a steady state with the exposure time. We hypothesize that this steady state is reached before reaction (2) starts taking place in the oxygen depleted a-ZTO:Al. Then, the free electrons produced in reaction (1) are used for the reduction of Sn and do not contribute anymore to the increase in N_e. The description above would apply for the samples treated at 50 °C or 100 °C. The rate constant values obtained from fitting are 3×10^{-3} s^{-1} and 1.8×10^{-2} s^{-1} for 50 °C and 100 °C T_s, respectively. For the samples treated at 200 °C the contribution from the second reaction occurs almost immediately after reaction (1) and therefore $\frac{d[N_e']}{dt}$ cannot be solely described by first-order reaction kinetics.

We have shown that a H_2 plasma treatment effectively improves the electrical properties of a-ZTO:Al by increasing the free-carrier concentration of the films. Controlling the reduction reaction rate by, for example, reducing the substrate temperature allows for this increase in free-carrier concentration while delaying the formation of large Sn metallic particles. The H_2-plasma treatment at 50 °C reduced the resistivity of a-ZTO:Al films from 9×10^{-3} to 3.8×10^{-3} Ω cm, with an increase of only 2% in optical absorptance.

The authors acknowledge the financial support from the European Union Seven Framework Program (FP7-ICT-2012, project number 314362) and from the Swiss National Science Foundation (SNSF) for partial support on equipment acquisition. M.M.-M. is grateful to B. Niesen, E. Moulin, and F. J. Haug for helpful discussions.

[1] K. Nomura, H. Ohta, A. Takagi, T. Kamiya, M. Hirano, and H. Hosono, Nature **432**, 488 (2004).
[2] D. H. Cho, S. Yang, C. Byun, J. Shin, M. K. Ryu, S. H. K. Park, C. S. Hwang, S. M. Chung, W. S. Cheong, S. M. Yoon, and H. Y. Chu, Appl. Phys. Lett. **93**, 142111 (2008).
[3] J. K. Jeong, S. Yang, D. H. Cho, S. H. K. Park, C. S. Hwang, and K. I. Cho, Appl. Phys. Lett. **95**, 123505 (2009).
[4] U. K. Kim, S. H. Rha, J. H. Kim, Y. J. Chung, J. Jung, E. S. Hwang, J. Lee, T. J. Park, J.-H. Choi, and C. S. Hwang, J. Mater. Chem. C **1**, 6695 (2013).
[5] S. W. Heo, Y. D. Ko, Y. S. Kim, and D. K. Moon, J. Mater. Chem. C **1**, 7009 (2013).
[6] T. Minami, H. Sonohara, S. Takata, and H. Sato, Jpn. J. Appl. Phys. **33**, L1693 (1994).
[7] Z. Chen, E. Wiedemann, and Q. Liu, "Wet etching of zinc tin oxide thin films," U.S. patent 0,075,421 A1 (2009).
[8] J. Lee, S.-C. Lee, C. S. Hwang, and J.-H. Choi, J. Mater. Chem. C **1**, 6364 (2013).
[9] C. H. Kim, Y. S. Rim, and H. J. Kim, ACS Appl. Mater. Interfaces **5**, 6108 (2013).
[10] W. H. Hlaing Oo, S. Tabatabaei, M. D. McCluskey, J. B. Varley, A. Janotti, and C. G. Van de Walle, Phys. Rev. B **82**, 193201 (2010).
[11] A. K. Singh, A. Janotti, M. Scheffler, and C. G. Van de Walle, Phys. Rev. Lett. **101**, 055502 (2008).
[12] C. G. Van de Walle, Phys. Rev. Lett. **85**, 1012 (2000).
[13] T. Koida, H. Shibata, M. Kondo, K. Tsutsumi, A. Sakaguchi, M. Suzuki, and H. Fujiwara, J. Appl. Phys. **111**, 063721 (2012).
[14] H.-R. Kim, D.-H. Kim, E. Byon, G.-H. Lee, G.-H. Lee, and P.-K. Song, Jpn. J. Appl. Phys. **49**, 121101 (2010).
[15] W. Korner, P. Gumbsch, and C. Elsasser, Phys. Rev. B **86**, 165210 (2012).
[16] D. M. Lee, J. K. Kim, J. C. Hao, H. K. Kim, J. S. Yoon, and J. M. Lee, J. Alloys Compd. **583**, 535 (2014).
[17] S.-H. Yang, J. Y. Kim, M. J. Park, K.-H. Choi, J. S. Kwak, H.-K. Kim, and J.-M. Lee, Surf. Coat. Technol. **206**, 5067 (2012).
[18] S.-H. Yang, D. M. Lee, J. Y. Kim, J. W. Kang, and J. M. Lee, J. Phys. D: Appl. Phys. **46**, 125103 (2013).
[19] H. R. Kim, G. H. Lee, and D. H. Kim, J. Phys. D: Appl. Phys. **44**, 185203 (2011).
[20] We suspect that the lower N_e of the sample treated at 200 °C is a result of the strongly modified surface of the films after the plasma treatment. The Hall effect measurements assume a homogeneous bulk film, however, the films treated at 200 °C are actually more accurately described as a multilayer composed of a discontinuous layer of Sn metal particles, a porous layer depleted of Sn and the bulk of the film. The plotted values for the sample treated at 200 °C, mainly for the treatment of 5 min, could therefore be influenced by this measurement artifact.
[21] See supplementary material at http://dx.doi.org/10.1063/1.4896051 for details on the effects of the surface metal particles on the optical properties of the film.
[22] M. Albrecht, R. Schewski, K. Irmscher, Z. Galazka, T. Markurt, M. Naumann, T. Schulz, R. Uecker, R. Fornari, S. Meuret, and M. Kociak, J. Appl. Phys. **115**, 053504 (2014).
[23] M. Schwind, V. P. Zhdanov, I. Zoric, and B. Kasemo, Nano Lett. **10**, 931 (2010).
[24] K. Nomura, T. Kamiya, and H. Hosono, ECS J. Solid State Sci. Technol. **2**, P5 (2013).
[25] F. Bekisli, M. Stavola, W. B. Fowler, L. Boatner, E. Spahr, and G. Lupke, Phys. Rev. B **84**, 035213 (2011).
[26] P. Agoston, K. Albe, R. M. Nieminen, and M. J. Puska, Phys. Rev. Lett. **103**, 245501 (2009).
[27] R. G. Pavelko, H. Daly, M. Hübner, C. Hardacre, and E. Llobet, J. Phys. Chem. C **117**, 4158 (2013).
[28] Q. Zhu, Q. Ma, D. B. Buchholz, R. P. H. Chang, M. J. Bedzyk, and T. O. Mason, J. Appl. Phys. **115**, 033512 (2014).
[29] L. Ding, S. Nicolay, J. Steinhauser, U. Kroll, and C. Ballif, Adv. Funct. Mater. **23**, 5177 (2013).
[30] T. B. Reed, *Free Energy of Formation of Binary Compounds* (MIT Press, Cambridge, MA, 1971).